



Cite this: *Chem. Commun.*, 2017, 53, 557

Received 20th November 2016,
Accepted 5th December 2016

DOI: 10.1039/c6cc09246b

www.rsc.org/chemcomm

$\alpha_v\beta_3$ -Isoform specific erbium complexes highly specific for bladder cancer imaging and photodynamic therapy†

Yan Zhou,^a Chi-Fai Chan,^b Daniel W. J. Kwong,^{*a} Ga-Lai Law,^{*b} Steven Cobb,^c Wai-Kwok Wong^{*a} and Ka-Leung Wong^{*a}

We have synthesized a bifunctional erbium–porphyrin tumor imaging and PDT agent (Er–R₃) that is capable of killing bladder cancer cells via its selective binding to the integrin $\alpha_v\beta_3$ isoform overexpressed on the cell membrane.

Photodynamic therapy (PDT) is an emerging novel cancer treatment modality suitable for repeated applications in treating diverse tumors. Since the treatment is highly localized, its systemic side-effects are relatively minimal with little adverse impact on the quality of life of the patients.¹ Despite these advantages and the approval of a number of photo-sensitizers by the US Food and Drug Administration in the 1980s as a treatment option for localized (*i.e.*, non-metastatic) cancers as well as for pre-cancerous lesions on skin and in the mouth, clinical use of PDT is still rather limited.² This is due partly to technological constraints and partly to a lack of recognition of PDT as a medical specialty.³ Recently, with significant advances in light delivery and imaging technology, we begin to see a renaissance of PDT research and clinical translation.^{4–7} Nevertheless, conventional PDT drugs still suffer from several drawbacks: (i) it is only able to treat those lesions where light can penetrate, *i.e.*, a few millimeters under the skin or from the irradiated tissue surface; (ii) some currently used PDT drugs render patients very sensitive to light and special precautions against light exposure must be taken until the drugs are cleared from the body in several days or even weeks; (iii) adverse *in vitro*/*in vivo* reactions occur due to the variation in physiological conditions and notched distribution of cytotoxic singlet oxygen; and (iv) non-specific cytotoxic activity may inflict damage to the normal cells during the PDT treatment.

Porphyrin-based compounds, the first-generation PDT drugs, have been investigated continuously since their first clinical

approval in an effort to overcome these drawbacks.^{8–10} Recently, several porphyrin derivatives have been developed to absorb strongly in the near-infrared (NIR) region ($\lambda > 800$ nm), where the tissue-penetration depth is much higher, *via* multi-photon femtosecond laser excitation with pinpoint accurate targeting to reduce collateral photodamage.^{11,12} In addition to the precise targeting using multi-photon laser, cancer selectivity can be incorporated into the PDT agents by taking advantages of some specific characteristics of the cancer cells. One recent example is a bifunctional gadolinium–porphyrin derivative which binds specifically to the anionic membrane of the cancer cells and then exerts its PDT action after NIR-excited imaging.¹³

Our design of a new generation bifunctional tumor-imaging and PDT agent is based on porphyrin–lanthanide complexes, with specific functional groups which allow them to localize selectively on particular tumor types, together with responsive imaging *via* NIR emission from the lanthanide.^{14,15} In this work, the tumor selective binding of the porphyrin–erbium complexes, **Er–R_n** ($n = 1–3$), is achieved through conjugation with bladder cancer-specific as well as integrin $\alpha_v\beta_3$ isoform-specific peptides. The bladder cancer-specific peptide sequences, **R₁–R₃** (molecular structures of **R₁–R₃** are shown in Scheme S2, ESI†), are obtained from a combinatorial chemistry approach, with **R₁** further reported to be $\alpha_v\beta_3$ integrin-specific as well.¹⁶ An increased integrin $\alpha_v\beta_3$ expression has been observed in the neovasculature of bladder cancer, particularly in invasive carcinoma.^{16–18} Our results show that **Er–R₃** is able to interrupt bladder tumor growth significantly with specific lysosome localization indicated by responsive emission from Er. To increase the water solubility of the Er complexes over our previously reported analogues,^{13,14} a hydrophilic peptide RrRK was conjugated to the relatively more hydrophobic bladder cancer-specific peptide sequence **R₂** (–cGRLKEKKc–), affording the amphiphilic **R₃** peptide with an improved cell membrane permeability. The absorption coefficients and emission quantum yields of **Er–R₁**, **Er–R₂** and **Er–R₃** are similar. The results of the photophysical measurement of **Ln–R_n** are shown in Table 1. Er exhibits stronger singlet oxygen quantum efficiency than Yb due to the fact that energy

^a Department of Chemistry, Hong Kong Baptist University, Kowloon Tong, Hong Kong SAR, China. E-mail: wkwong@hkbu.edu.hk, klwong@hkbu.edu.hk

^b Department of Applied Biology and Chemical Technology, Hong Kong Polytechnic University, Hung Hum, Hong Kong SAR, China

^c Department of Chemistry, Durham University, Durham, DH1 3LE, UK

† Electronic supplementary information (ESI) available. See DOI: 10.1039/c6cc09246b



Table 1 Summary of photophysical properties of **Ln-R_n** (Ln = Yb, Er; *n* = 1, 2, 3)

Compound	Absorption ^a (λ_{max}) [nm] log(ϵ [dm ³ mol ⁻¹ cm ⁻¹])	Emission ^a (λ_{em}) [nm] ($\Phi = \tau$) ^{b,c}	Φ_{Δ} ^d
Yb-R₁	425(5.37), 554(4.09)	656, 712(0.012), 975(29.86 μ s)	Not found
Yb-R₂	425(5.34), 554(4.16)	656, 712(0.013), 975(30.08 μ s)	Not found
Yb-R₃	425(5.27), 554(4.04)	656, 712(0.013), 975(29.97 μ s)	Not found
Er-R₁	426(5.32), 554(4.05)	654, 715(0.014), 1531	0.11
Er-R₂	426(5.50), 554(4.53)	654, 715(0.014), 1531	0.12
Er-H₃	426(5.36), 554(4.24)	654, 715(0.015), 1531	0.12

^a Absorption and emission were measured in water (3% DMSO) at room temperature. ^b The emission quantum yield standard used was tetraphenylporphyrin (H₂TPP) in anhydrous DCM ($\Phi_{\text{em}} = 0.120$ at 298 K). ^c Lifetime was measured in water (3% DMSO) at room temperature.

^d The singlet oxygen quantum yield measured was referenced to tetraphenylporphyrin (H₂TPP) in anhydrous DCM ($\Phi_{\Delta} = 0.62$ at 298 K).

transfer from porphyrin to Yb for f-f emission is much better than that to Er for f-f emission, resulting in more excitation energy being channeled to singlet oxygen production.

In Fig. 1, the photophysical properties of Er or Yb porphyrin-based complexes are similar. However, the *in vitro* subcellular localization uptake and cytotoxicity (light and dark) are different due to the conjugated peptides. First of all, the subcellular localizations of **Er-R_n** and **Yb-R_n** complexes (*n* = 1, 2 and 3) in bladder cancer 5637 and T24 cells, cervical cancer HeLa cells and normal lung MRC5 cells (Fig. 2 and Fig. S24, ESI[†]) are different (dosed concentration = 5 μ M; incubation time = 6 hours). The *in vitro* fluorescence intensity of the three Er complexes is higher than those of their Yb counterparts. This is due to an efficient energy transfer from the porphyrin to the Yb³⁺ ion

which emits in the near-infrared region. In the bladder cancer 5637 and T24 cells, red porphyrin emission from **Er-R₁** is found only on the cell membrane, while the red emissions from **Er-R₂** and **Er-R₃** are found inside the cells. Their Yb analogues also showed the same subcellular localization pattern, *i.e.*, the porphyrin emission from **Yb-R₁** is found on the cell membrane while **Yb-R₂** and **Yb-R₃** are found within the cells. Co-localization experiments using green LysoTracker were conducted. The red emissions from **Er-R₂**, **Er-R₃**, **Yb-R₂** and **Yb-R₃** were observed to overlap well with the green fluorescence from the LysoTracker in the 5637 and T24 cells (Fig. S22, ESI[†]). No such overlap was seen with **Er-R₁** and **Yb-R₁**. These observations clearly indicate that the **Er-R₂**, **Er-R₃**, **Yb-R₂** and **Yb-R₃** complexes are mostly localized in the lysosomes of the 5637 and T24 cells. **Er-R₁** and **Yb-R₁**, however, are localized in the 5637 and T24 cell membrane. This is consistent with the reported specificity of the conjugated **R₁** peptide towards integrin $\alpha_v\beta_3$ over-expressed on the bladder cancer cell membrane.

To confirm that the peptide sequences **R₁**, **R₂** and **R₃** recognize bladder cancer specifically, *in vitro* imaging of **Er-R_n** and **Yb-R_n** (*n* = 1, 2 and 3) was performed using the non-bladder cancer cells, HeLa and MRC-5, under identical experimental conditions. No red emission was detected in HeLa or MRC-5 cells, thus showing very limited uptake of these porphyrin-lanthanide complexes. As the porphyrin complexes **Er-R_n** and **Yb-R_n** (*n* = 1, 2 and 3) will not bind to HeLa and MRC-5 cells, only the green emission from the LysoTracker is observed in the fluorescence staining experiment (Fig. S22, ESI[†]).

To confirm that the selective uptake of **Er-R_n** and **Yb-R_n** (*n* = 1, 2 and 3) complexes by bladder cancer cells was due to the recognition of the $\alpha_v\beta_3$ integrin on the 5637 and T24 cell surface, cellular uptake of these complexes functionalized with different peptides **R₁**, **R₂** and **R₃** was studied by flow cytometry on the 5637, T24, HeLa and MRC-5 cells. Both **R₁** and **R₂** peptides were shown to exhibit specific binding towards bladder cancer through screening using the one-bead one-compound (OBOC) combinatorial peptide library technology,¹⁹ with **R₁** further reported to bind to the $\alpha_v\beta_3$ integrin on the T24 cell. The bladder cancer-specific binding of **R₁** was further demonstrated *in vivo* on a xenograft mouse model.²⁰ **R₃** is designed as an amphiphilic peptide modified from **R₂** by the addition of a hydrophilic peptide RrRK to its N-terminal to enhance its cell permeability. The results from the flow cytometric cell uptake experiments are shown in Fig. S23 (ESI[†]). From Fig. S23 (ESI[†]),

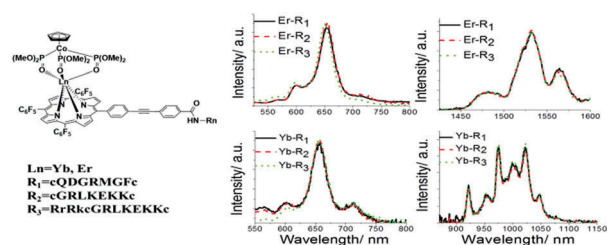


Fig. 1 (left) Molecular structures of **Ln-R_n**, (middle) visible and (right) near-infrared emission spectra of **Ln-R_n** in aqueous solution with 430 nm excitation (conc. = 1 μ M, Ln = Er or Yb, *n* = 1, 2 and 3).

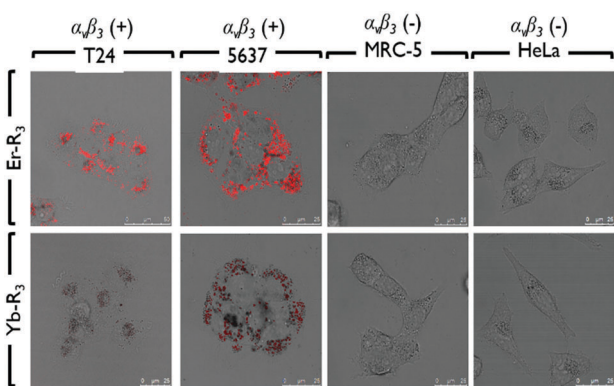


Fig. 2 Subcellular localization of **Er-R₃** and **Yb-R₃** in human bladder carcinoma (T24 and 5637) cells, normal lung fibroblast (MRC-5) cells, and human cervical carcinoma (HeLa) cells.



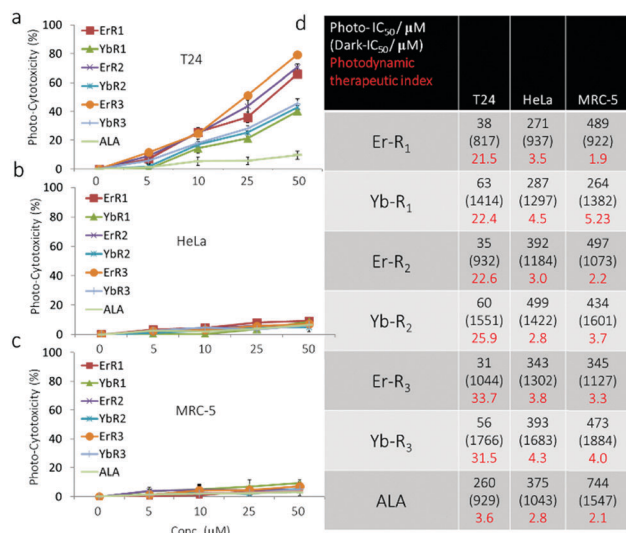


Fig. 3 Comparison of *in vitro* photo-cytotoxicity of **Er-R_n** and **Yb-R_n** porphyrin complexes with ALA in (a) T24, (b) HeLa and (c) MRC-5 cells irradiated at 10 J cm⁻² using a 550 nm long-pass filter. (d) Summary of the IC₅₀ value of **Er-R_n** and **Yb-R_n** porphyrin complexes and ALA in the presence and absence of irradiation in T24, HeLa and MRC-5 cells.

no significant uptake of the **Er-R_n** and **Yb-R_n** ($n = 1, 2$ and 3) complexes is observed in HeLa and MRC-5 cells even after 24 hours of incubation. In contrast, substantial uptake of these complexes by the 5637 and T24 cells is clearly seen after 6 hours of incubation. Regarding the Er and Yb complexes functionalized with different peptides, their uptake rates by the 5637 and T24 cells showed the following trend: **R₃** > **R₂** > **R₁**. This observation is also reflected in the median fluorescence intensity recorded for these complexes after 24 hours of incubation (Table S2, ESI†).

After verifying the specific uptake of **Er-R_n** and **Yb-R_n** complexes into T24 cells, *in vitro* PDT in various cell lines was carried out. A clinically approved conventional PDT agent, aminolevulinic acid (ALA), which exhibits no specific tumor selectivity, was used for comparison as well.²¹ An ideal PDT photosensitizer should have a low dark cytotoxicity (*i.e.*, a high dark IC₅₀) and a high photo-cytotoxicity (*i.e.*, a low light IC₅₀).

These two contrasting properties can be summarized in terms of a photodynamic therapeutic index, PTI, which is defined as the ratio of the dark IC₅₀ over light IC₅₀ of the PDT agent. The cytotoxicity of **Er-R_n** and **Yb-R_n** complexes towards T24, HeLa and MRC-5 cells was measured in dark and under photo-irradiation (550 nm long-pass filter, 6 mW cm⁻², 28 min) using MTT assay. The results are shown in Fig. 3. These complexes exhibited high photo-cytotoxicity under a light dose of 10 J cm⁻². Furthermore, their photo-cytotoxicity increased with increasing concentrations of the **Er-R_n** and **Yb-R_n** complexes. The IC₅₀ of **Er-R_n** and **Yb-R_n** complexes to the T24 cells is 8–10 fold lower than those towards the HeLa and MRC-5 cells, thus demonstrating their selective PDT activities towards bladder cancer. Due to the amphiphilic character of the **R₃** peptide in **Er-R₃** and **Yb-R₃**, the cellular uptake of these complexes is higher than those of

Er-R₁, **Er-R₂**, **Yb-R₁** and **Yb-R₂**, thus resulting in their higher photo-cytotoxicity. In comparison, the ALA-PDT activity towards the T24 cells is 4–8 fold lower than those of the **Er-R_n** and **Yb-R_n** complexes. As for the HeLa and MRC-5 cells, ALA showed photo-cytotoxicity either comparable to or lower than those of the **Er-R_n** and **Yb-R_n** complexes. Among all of the **Er-R_n** and **Yb-R_n** complexes, **Er-R₃** shows the highest PTI of *ca.* 34, followed by **Er-R₂** > **Er-R₁**. A similar trend is seen with the **Yb-R_n** complexes: **Yb-R₃** > **Yb-R₂** > **Yb-R₁**. The dark cytotoxicity of all these complexes is very low (with their dark IC₅₀ of over 1000 μM). Based on these results, **Er-R₃** is the most promising candidate as a new generation PDT agent to selectively kill bladder cancer. Since a peptide specific for a particular cancer or stem cell type can be identified from a phage-displayed random peptide,^{22–24} our new generation erbium porphyrin complex can be extended not only to targeted imaging and destruction of any cancer type but also to tracking stem cell migration.

In conclusion, we present a multi-modal lanthanide-porphyrin PDT agent that is capable of killing tumor cells *via* ¹O₂ produced from a porphyrin moiety, affording fluorescence imaging simultaneously. **Er-R₃** is synthesized, and it shows high selectivity for bladder cancer cells by specifically targeting the integrin α_vβ₃ isoform with strong NIR emission and ¹O₂ generation. The selective uptake of our complexes by cancer cells is confirmed by flow cytometry and *in vitro* imaging, and they are able to significantly interrupt the growth of bladder cancer cells *via* specific binding to the “integrin α_vβ₃ isoform”.

This work was supported by the Hong Kong Baptist University (HKBU) Faculty Research Grants (FRG2/14-15/013), the Hong Kong Polytechnic University (HKPolyU), the Hong Kong Research Grants Council (HKBU 22301615, Polyu 253002/14P and Polyu 5096/13P) and the HKBU-HKPolyU Joint Research Programme (RC-ICRS/15-16/02F-KLW and RC-ICRS/15-16/02D-DWJK).

Notes and references

1. I. Yoon, J. Z. Li and Y. K. Shim, *Clin. Endosc.*, 2013, **46**, 7–23.
2. D. E. J. G. J. Dolmans, D. Fukumura and R. K. Jain, *Nat. Rev. Cancer*, 2003, **3**, 380–387.
3. K. Moghissi, *Photodiagn. Photodyn. Ther.*, 2011, **8**, 73–74.
4. J. Chen, L. Keltner, J. Christophersen, F. Zheng, M. Krouse, A. Singhal and S.-S. Wang, *Cancer J.*, 2002, **8**, 154–163.
5. S. Mordon, C. Cochrane, J. B. Tylcz, N. Betrouni, L. Montier and V. Koncar, *Photodiagn. Photodyn. Ther.*, 2015, **12**, 1–8.
6. T. Nakamura, T. Oinuma, H. Yamagishi, H. Masuyama and A. Terano, *Photodiagn. Photodyn. Ther.*, 2015, **12**, 115–122.
7. H. Lee, Y. Lee, C. Song, H. R. Cho, R. Ghaffari, T. K. Choi, K. H. Kim, Y. B. Lee, D. Ling, H. Lee, S. J. Yu, S. H. Choi, T. Hyeon and D.-H. Kim, *Nat. Commun.*, 2015, **6**, 10059.
8. L. G. Arnaut, *Adv. Inorg. Chem.*, 2011, **63**, 187–233.
9. M. Ethirajan, Y. Chen, P. Joshi and R. K. Pandey, *Chem. Soc. Rev.*, 2011, **40**, 340–362.
10. V. Bogoeva, M. Siksjø, K. G. Saeterbo, T. B. Melo, A. Bjorkoy, M. Lindgren and O. A. Gederaas, *Photodiagn. Photodyn. Ther.*, 2016, **14**, 9–17.
11. E. Dahlstedt, H. A. Collins, M. Balaz, M. K. Kuimova, M. Khurana, B. C. Wilson, D. Phillips and H. L. Anderson, *Org. Biomol. Chem.*, 2009, **7**, 897–904.
12. C.-T. Poon, P.-S. Chan, C. Man, F.-L. Jiang, R. N. S. Wong, N.-K. Mak, D. W. J. Kwong, S.-W. Tsao and W.-K. Wong, *J. Inorg. Biochem.*, 2010, **104**, 62–70.
13. T. Zhang, R. Lan, C.-F. Chan, G.-L. Law, W.-K. Wong and K.-L. Wong, *Proc. Natl. Acad. Sci. U. S. A.*, 2014, **111**, E5492–E5497.



- 14 T. Zhang, C.-F. Chan, J. Hao, G.-L. Law, W.-K. Wong and K.-L. Wong, *RSC Adv.*, 2013, **3**, 382–385.
- 15 G. L. Law, R. Pal, L. O. Palsson, D. Parker and K.-L. Wong, *Chem. Commun.*, 2009, 7321–7323.
- 16 M. D. Sachs, K. A. Rauen, M. Ramamurthy, J. L. Dodson, A. M. De Marzo, M. J. Putzi, M. P. Schoenberg and R. Rodriguez, *Urology*, 2002, **60**, 531–536.
- 17 S. Liu, S. P. Robinson and D. S. Edwards, *Top. Curr. Chem.*, 2005, **252**, 193–216.
- 18 T. Saito, M. Kimura, T. Kawasaki, S. Sato and Y. Tomita, *Br. J. Cancer*, 1996, **73**, 327–331.
- 19 H. Zhang, O. H. Aina, K. S. Lam, R. de Vere White, C. Evans, P. Henderson, P. N. Lara, X. Wang, J. A. Bassuk and C. X. Pan, *Urol. Oncol.*, 2012, **30**, 635–645.
- 20 T. Y. Lin, H. Zhang, S. Wang, L. Xie, B. Li, C. O. Rodriguez, R. de Vere White and C. X. Pan, *Mol. Cancer*, 2011, **10**, 9.
- 21 M.-C. Tetard, M. Vermandel, S. Mordon, J.-P. Lejeune and N. Reyns, *Photodiagn. Photodyn. Ther.*, 2014, **11**, 319–330.
- 22 G. Abbineni, S. Modali and C. Mao, *Mol. Pharmaceutics*, 2010, **7**, 1629–1642.
- 23 N. Gandra, G. Abbineni and C. Mao, *Small*, 2013, **9**, 215–221.
- 24 K. Ma, D. Wang, Y. Lin and C. Mao, *Adv. Funct. Mater.*, 2013, **23**, 1172–1181.

